Indian Journal of Engineering & Materials Sciences
Vol. 11, February 2004, pp. 31-37

Analysis of reacting flows in an aero-engine afterburner using computational fluid dynamics

Sunil V Unaune & V Ganesan

Internal Combustion Engines Laboratory, Department of Mechanical Engineering, Indian Institute of Technology, Chennai 600 036, India

Received 4 February 2003; accepted 16 December 2003

In this paper, reacting flows in an aero-engine afterburner are analyzed using computational fluid dynamics (CFD). A computational procedure is described for calculating the three-dimensional reacting flow fields in a gas turbine afterburner. The computations are based on numerical solution of time-averaged transport equations for mass, momentum, turbulent kinetic energy and dissipation rate using a finite volume formulation. The numerical calculations are performed using SIMPLE (Semi Implicit Method for Pressure Linked Equations). The RNG (Re-normalization Group Theory) k-ε model is used for turbulence modeling. Combustion is modeled using PDF (Probability Density Function). The results for air-fuel ratio of 30 and 46 are obtained and analyzed.

In aircraft applications, larger thrust for a small duration is required sometimes. This can be achieved in two ways. One way is to increase the mass flow rate. The other way is to add energy by burning additional fuel in the tail pipe between turbine exhaust and the entrance section of the exhaust nozzles. This way of thrust augmentation is called afterburning and the device is called the afterburner. Due to the ever increasing demand for thrust, especially in military aircrafts, afterburner seems to be the most practical method during such flight operations. Some investigations[1-5] provide details about the flow and flame studies of systems applied to afterburners and flame stabilization that are close to afterburning systems. In modern theoretical analysis, CFD plays a major part and its details are also known[6-10].

Useller[11] presented the results of several full-scale turbojets–engine afterburner investigations that have been conducted by NASA. Considering combustion efficiency as a criterion of the afterburner performance, effect of combustion chamber length on afterburner combustion performance was experimentally determined. Macquisten and Dowling[12] investigated low frequency combustion oscillations in a model afterburner. An experimental rig with a conical gutter flame stabilizer was run for a range of inlet Mach numbers and temperatures representative of an engine afterburner. Baxter and Lefebvre[13] conducted experiments on bluff body flame stabilization to obtain weak extinction limit data from an apparatus designed to simulate the characteristics of practical afterburner combustion system. Kumar[14] proposed a method to estimate pressure loss across flameholders in high velocity streams. Experiments were carried out in a 20 inch diameter afterburner fitted with an anti-screech liner and spray bars for fuel injection. Ganesan[15] predicted the turbulent flow behind a conical baffle using finite difference prediction procedure. The flow was assumed to be 2D axisymmetric, steady, turbulent and non-reacting. Governing differential equations, together with boundary conditions were solved by finite-difference method based on SIMPLE algorithm. Zhang and Chiu[16] developed a numerical method and computer code for modeling afterburner spray combustion and gas phase combustion processes, based on the Navier-Stokes equations and finite difference method. Chuang and Jiang[17] analyzed diffusion flame in an afterburner as a function of air-fuel ratio by employing SIMPLE-C algorithm and k-ε model for turbulence. In order to simulate practical afterburner flow, two open-mouth-type V-gutters were considered instead of a solid cone as employed by Zhang and Chiu[16].

Theoretical

Schematic of an afterburner shown in Fig. 1 consists of an exhaust diffuser with struts, fuel manifolds, flame stabilizer, combustion chamber with anti-screech holes and cooling rings and variable area nozzle. Liquid fuel is added through fuel manifolds and

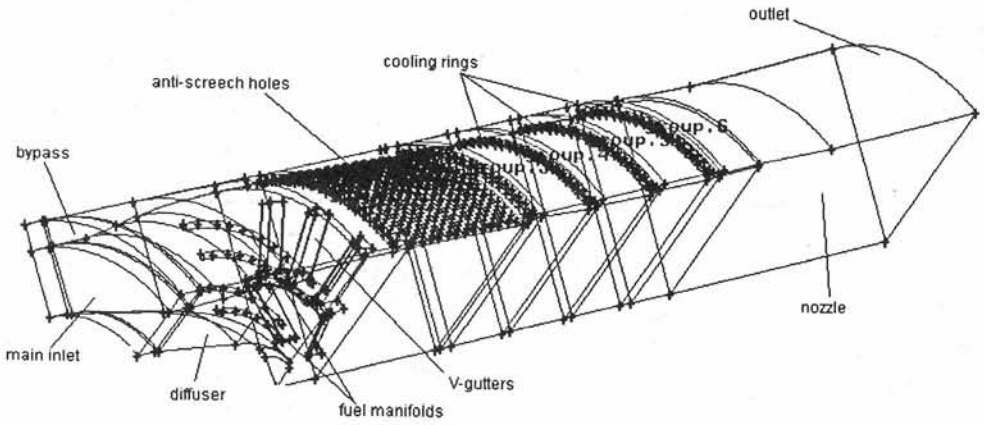

Fig. 1 — Geometry of the afterburner (60° sector)

the combustion process is initiated in the wakes created by the flame stabilizer. The core flow leaving the turbine is de-swirled and is decelerated in the diffuser. The mixing further depends on turbulence created by v-gutter, the distance between the v-gutter and fuel manifolds, the method of injection of fuel etc. Further, the entrainment within the re-circulation zone plays a key role in the sustained combustion process. So, it is necessary to carry out a detailed study involving various parameters affecting mixing and combustion.

Governing equations

There are seven unknowns namely pressure, temperature, density, velocities along the three co-ordinate axes and internal energy for fluid. Now, seven governing equations are required to solve the problem. These governing equations are continuity, momentum equations in three co-ordinate axes, energy equation, two equations of state.

Continuity equation

$$\frac{\partial}{\partial X_i}(\rho u_i) = S_m$$

where u_i is the mean velocity component and S_m is the source of the mass added to the continuous phase due to the vaporization of fuel droplets.

Momentum equation in x-direction

$$\frac{\partial}{\partial X_j}(\rho u_i u_j) = -\frac{\partial p}{\partial X_i} + \frac{\partial \tau_{ij}}{\partial X_j} - \frac{\partial}{\partial X_j}(\frac{2}{3}\rho k \delta_{ij}) + F_i$$

where $\tau_{ij} = \left[\mu_{eff}\left(\frac{\partial u_i}{\partial X_j} + \frac{\partial u_j}{\partial X_i} - \frac{2}{3}\delta_{ij}\frac{\partial u_i}{\partial X_i}\right)\right]$

The effective viscosity μ_{eff} is the sum of turbulent viscosity μ_t and laminar viscosity μ_l, p is the static pressure, k the turbulent kinetic energy and F_i is the external body force that arises from interaction with the dispersed phase in the i direction. The turbulent viscosity is obtained from the turbulent kinetic energy k and dissipation rate ε.

$$\mu_t = \rho C_\mu \frac{k^2}{\varepsilon}$$

where C_μ= 0.0845. k and ε are obtained from the solution of their transport equations which are derived from the RNG theory.

Energy equation

$$\frac{\partial}{\partial t}(\rho H) + \frac{\partial}{\partial X_i}(\rho u_i H) = \frac{\partial}{\partial X_i}\left(\frac{k_t}{C_p}\frac{\partial H}{\partial X_i}\right) + \tau_{ik}\frac{\partial u_i}{\partial X_k} + S_h$$

where H is the total enthalpy and S_h is the source of energy due to chemical reaction.

Combustion modeling

Combustion phenomena have been modeled using probability density function (PDF) approach. PDF approach is good for turbulent diffusion flames[18]. Fuel is injected in the primary zone where it mixes with the oxidizer and burns. So, the flame is just like the turbulent diffusion flame. In PDF approach transport equations for two conserved scalars (the mean mixture fraction and its variance) are solved and individual component concentrations are derived from the predicted mixture fraction distribution. Here the turbulence effects are accounted for with the help of a probability density function. Equilibrium chemistry

model is used during PDF calculations. This chemistry model assumes that chemical equilibrium always exists at molecular level. An algorithm based on the minimization of Gibbs free energy is used to compute species mole fractions from mean mixture fraction. Thus value of any averaged scalars (e.g. temperature, density, etc.) depends upon mean mixture fraction, its variance and the chemistry model[19].

For non-adiabatic system, it depends upon instantaneous enthalpy also. Hence the solver solves the transport equation for instantaneous enthalpy also. PDF look-up table contains the values of different scalars for different combinations of mean mixture fraction, its variance and enthalpy.

Turbulence modeling

Flow through afterburner is highly turbulent. Averaged Navier-Stroke equation for turbulent flow has six additional stresses called Reynolds stresses. Now, if the turbulent viscosity is calculated or expressed in terms of any known variable, Reynolds stresses can be calculated. Turbulent models develop computational procedures to predict turbulent viscosity (or Reynolds stresses directly). As the flow through afterburner has swirl component at inlet, RNG k-ε model is used for turbulence modeling to take care of the swirl effect. RNG k-ε model is also good for low Reynolds number flows[18].

Pressure-velocity coupling

Semi Implicit Method for Pressure Linked Equation (SIMPLE) algorithm is used for pressure-velocity coupling. SIMPLE-algorithm is straightforward and has been successfully implemented in numerous CFD procedures. It produces correct velocity field[20]. Under-relaxation factors are used to avoid the divergence. By trial and error method under-relaxation factors are selected for convergence.

For solving the governing equations of fluid flow, integration over all the control volumes of the solution domain is taken. Discretisation converts the integral equation into a system of algebraic equations. In order to solve these algebraic equations we need to calculate the transport property at the cell faces. So, the first order upwind differencing scheme is used. One of the major inadequacies of the central differencing scheme is its inability to identify the flow direction. Velocities in the afterburner are quite high. Hence flow direction should be considered while calculating the transport properties at the cell faces, which the upwind differencing scheme does. The analysis has been carried out at sea level operating conditions.

Grid generation

Pre-processor GAMBIT has been adopted for geometric modeling of afterburner. Only 60° sector of the afterburner is modeled for analysis so as to exploit the symmetry in the geometry. An unstructured grid of size 8,30,678 cells has been used for meshing. Fig. 2 shows the radial and ring V-gutters used for flame stabilization. There are 18 top and 6 bottom radial V-gutters.

The main objective of present work is to study reacting flows in afterburner. Results for air-fuel ratios of 30 and 46 are obtained and analyzed.

Fig. 3 shows different boundaries of the domain under consideration. The boundary conditions used at above boundaries are given in Table 1.

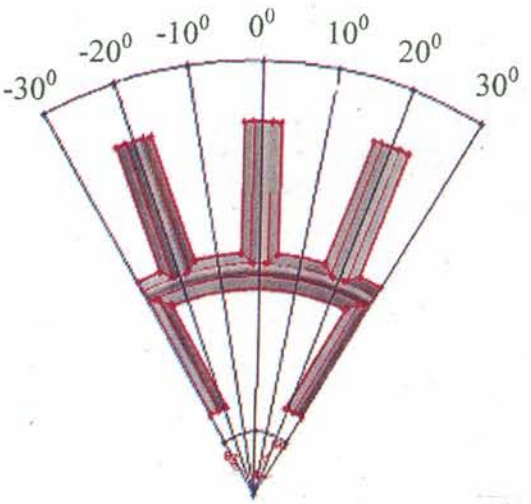

Fig. 2 — Radial and ring V-gutter

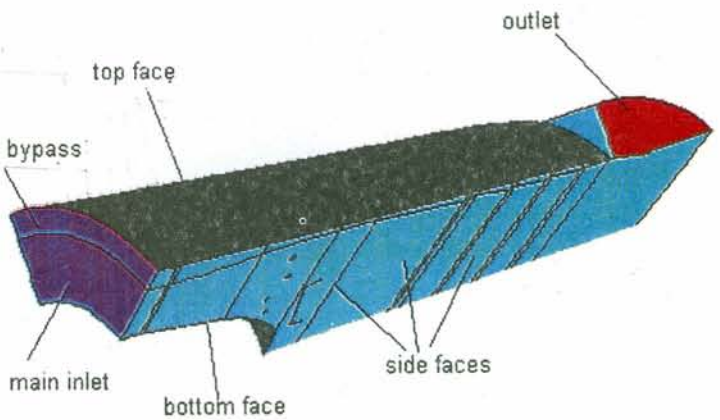

Fig. 3 — Boundaries of the domain

The main input conditions are: Air-fuel ratio (in primary zone) (30 and 46); Sauter mean diameter (18.5 μ); Fuel injection velocity (30 m/s); Temperature of fuel (300 K).

Results and Discussion

Figs 4 and 5 show the velocity contours at 0° plane for air-fuel ratio of 30 and 46 respectively from inlet to exit. A low velocity region can be observed behind the top gutter while the velocity is seen increasing near the top region where the bypass air enters through screech rings. The dark blue (or black if printed in black and white) regions indicate the effect of the wall in reducing the velocity while maximum velocity can be seen to be at the exit of the nozzle. Velocity is reduced from 250 m/s to 170 m/s in the diffuser. The bypass along the nozzle liner can be observed from the figure. Velocity is seen to be increasing as the flow approaches the nozzle. This is due to the expansion of gases resulting from high temperature.

The flow field velocity vectors behind the top gutter are shown in Fig. 6. The top portion of the gutter shows the formation of eddy with clockwise rotation due to the separation of flow at the top end of the gutter resulting in a sharp change in direction of flow. In the rest of the gutter the flow seems to have more or less anticlockwise motion. However, the flow phenomenon is quite complex in the middle region where the mixing of the flow from top and bottom portion of the gutter occurs. The complexity of the flow phenomenon in and around the gutter can be attributed to the volume expansion due to heat addition and the production of species due to combustion.

Fig. 7 shows the anchoring of flame at the gutter. High temperature regions are found in the top and

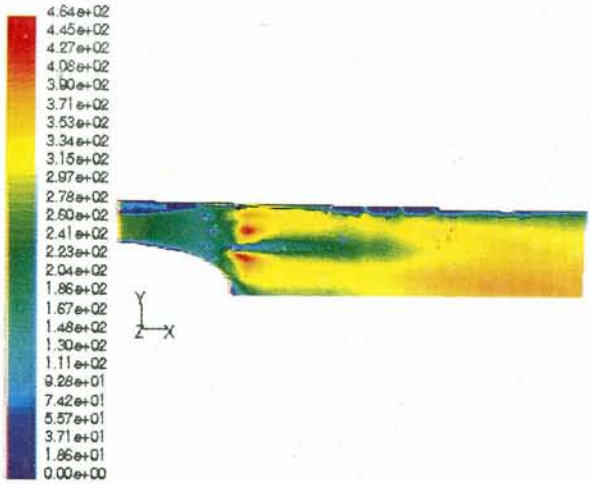

Fig. 4 — Contours of velocity magnitude for air-fuel ratio of 30

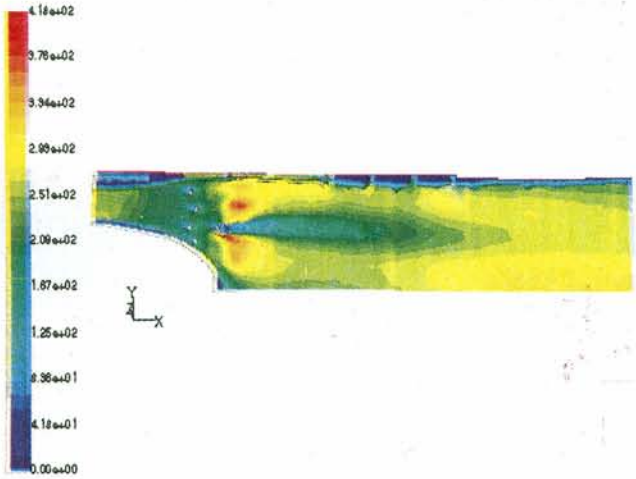

Fig. 5 — Contours of velocity magnitude for air-fuel ratio of 46

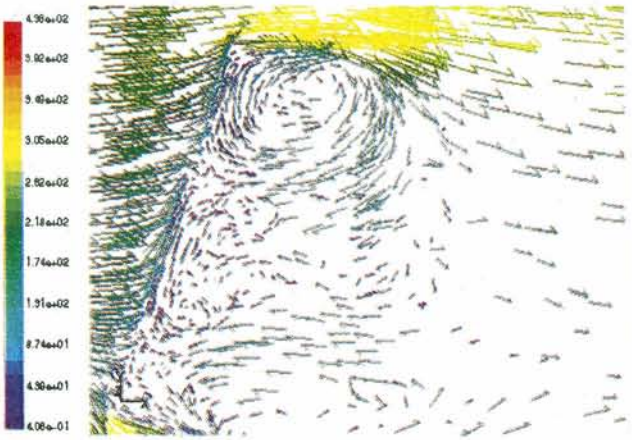

Fig. 6 — Re-circulation zone behind top gutter

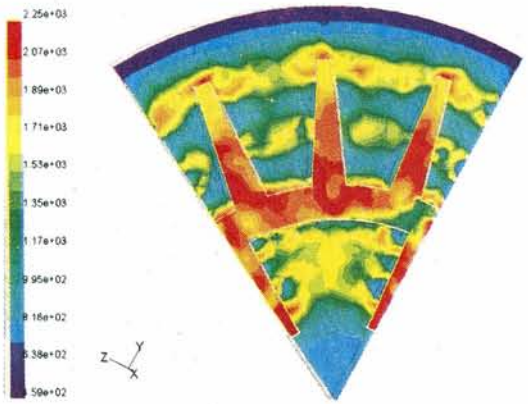

Fig. 7 — Total temperature contours at gutter cross section

bottom radial gutters along with the ring gutter. Thus all the gutters are instrumental in stabilizing the flame. Initiation of combustion just upstream of the gutter can be observed from the figure. This can be attributed to the fact that some amount of fuel in the fuel streams during their travel towards the gutter from the fuel manifolds evaporates and mixes with the air much before passing through the gutter. Since, the conducive temperature field is available the mixture starts combusting. However, completeness in combustion may be noticed in the wake region of the gutter where the temperature reaches maximum value (2246K).

Fig. 8 shows three-dimensional view of the gutter with fuel particle streams colored by particle residence times. The ring gutter and some portions of the top and bottom gutters intercept the fuel streams, which get diverted while the remaining pass through the gap between the gutters.

The residence time of the streams is maximum ahead of the gutter in the RC zone thus resulting in anchoring of flame. In Fig. 9 it can be seen that the streams striking the gutter result in cooling of gutter surface due to latent heat of vaporization of fuel, while the hot spots on the gutter back surface are the result of initiation of combustion of the mixture upstream of the gutter, which is shown by red spots. Thus, it may be seen that the gutter is successfully blocking the high velocity stream of air-fuel mixture to stabilize the flame.

Figs 10 and 11 show the static temperature contours for air-fuel ratio of 30 and 46 from entry to exit of the afterburner.

It is observed that flame anchors well at the gutter and the high temperature region is continuous till the exit. However, the liners are seen to be at much lower temperatures, due to the cooling effect produced by the bypass air. Some hot spots are observed on the fuel manifolds. But the maximum temperature is within the limit. On the top and bottom gutters, some

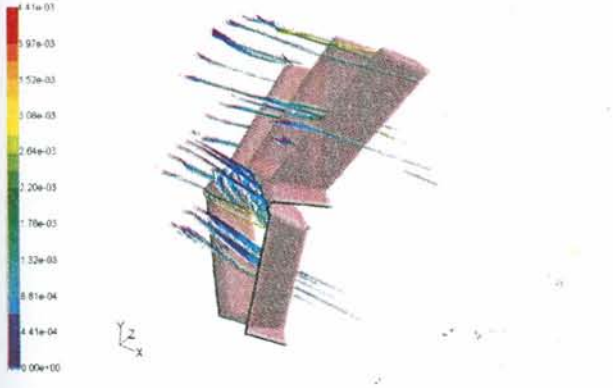

Fig. 8 — Gutter with particle streams colored by particle residence time

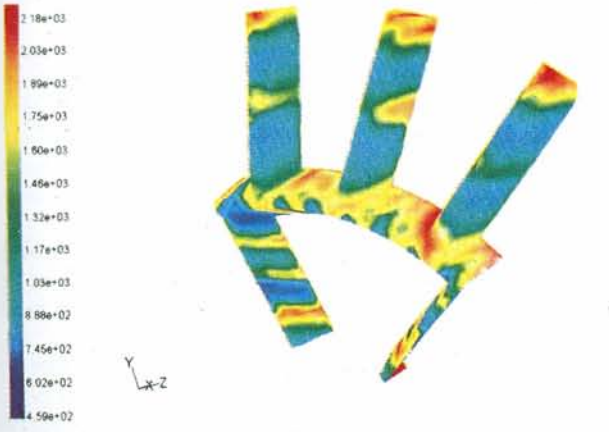

Fig. 9 — Total temperature contours (gutter back surface)

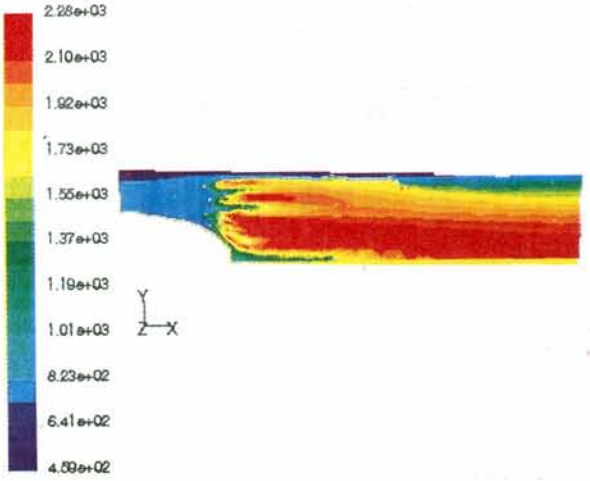

Fig. 10 — Contours of static temperature for air-fuel ratio of 30

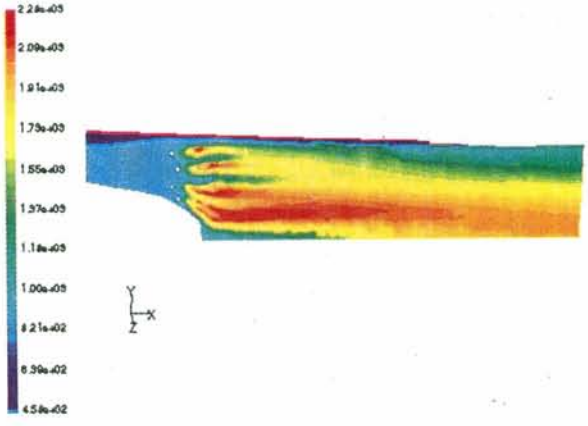

Fig. 11 — Contours of static temperature for air-fuel ratio of 46

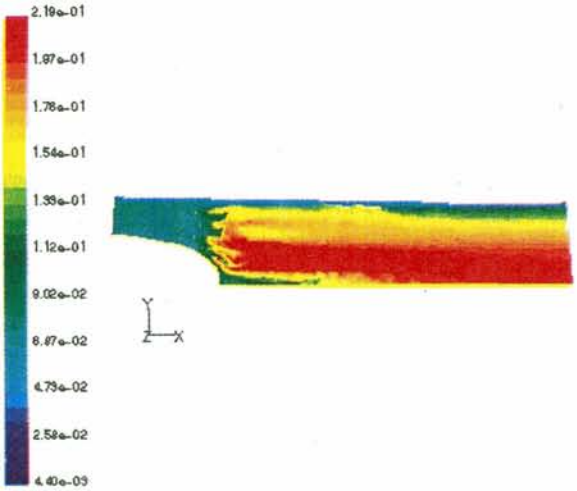

Fig. 12 — Contours of CO_2 mass fraction

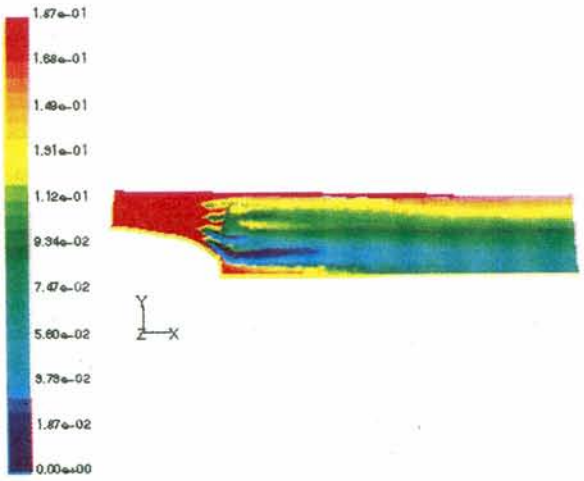

Fig. 13 — Contours of O_2 mass fraction

regions of maximum temperature are observed. That may be due to flame stabilization. As compared to the radial V-gutters, ring gutters seem to experience lower temperature. Due to the cooling air, liner temperature is also within limit. Some cooling air is bypassed to nozzle liner. The average temperature at nozzle outlet is 1500 K, while the maximum temperature of nozzle liner is 1000K, which shows the effect of bypass air. Fig. 12 shows the contours of CO_2 mass fraction at the central plane whereas Fig. 13 shows the contours of O_2 mass fraction for an air-fuel ratio of 30.

Contours of static temperature and CO_2 mass fraction are nearly complementary. This is because maximum temperature is the indication of complete combustion causing higher CO_2 production. So CO_2 mass fraction will be maximum where temperature is maximum. Regions of maximum temperature and CO_2 mass fraction have minimum O_2 mass fraction. This is due to utilization of O_2 for combustion. Thus, analyzing species fraction, one can obtain the state of combustion. From the total pressure contours (not given in this paper) it is seen that increasing air-fuel ratio decreased total pressure losses.

Conclusions

During the present investigations, CO_2 and O_2 fraction is found to be as expected at outlet. This indicates that combustion is complete.

Temperature of liners has been found to be within permissible limit. Also, temperature of nozzle liner is found to be less than average temperature at exit. This reveals that bypass air is cooling the nozzle liner effectively. Maximum temperature at the exit is less than the average temperature variation for the two air-fuel ratios studied.

Air-fuel ratio of 13 gives better afterburner performance as the pressure loss is within the design limit. Since the system is quite complex, experimental validation was not possible. However, to gain more confidence validation must be attempted.

References

1 Ravichandran M & Ganesan V, *IE (I) J-MC*, 77 (1996) 67-75.

2 Frolov S M, basevich V Ya & Belyaev A A, *Modeling of bluff-body stabilized combustion with detailed chemistry* (N.N.Semenov Institute of Chemical Physics, Moscow), 1999.

3 Bakrozis A G, Papailiou D D & Koutmos P, *Combust Flame*, 119 (1999) 291-306.

4 Suresh D, *Modeling of isothermal and reacting flows in gas turbine afterburners*, M.S. Thesis, I.C. Engines Laboratory, I.I.T. Madras, 2001.

5 FLUENT 5, *User's Guide, Vols 2& 3* (Fluent Incorporated, India), 1998.

6 Henderson R E & Blazowski W S, *Turbo propulsion combustion technology: Comprehensive study of aircraft gas turbine engines*, Part II, Chapter 20, AFAPL-TR-78-52, Air Force Aero Propulsion Laboratory, Wright-Patterson Air Force Base, Ohio, 1978.

7 Cohen H, Rogers G F C & Saravanamuttoo H I H, *Gas turbine theory* (Longman Group Ltd, USA), 1998.

8 Versteeg H K & Malalasekera W, *An introduction to computational fluid dynamics: The finite volume method* (Longman Group Ltd, UK), 1995.

9 Shaw C T, *Using computational fluid dynamics*, (Prentice Hall, USA), 1992.

10 Lefebvre A H, *Gas turbine combustion* (Hemisphere Publishing Corporation, New York), 1993.

11 James W Useller, *Effect of combustor length on afterburner combustion*, (Lewis Research Center, NASA), 1959.

12 Macquisten M A & Dowling A P, *Combust Flame*, (1993) 253-264.

13 Baxter M R & Lefebvre A H, *J Eng Gas Turbine Power*, 114 (1992), 776-781.
14 Kumar R K, *Combustion Sci Technol*, 21 (1980) 199-203.
15 Ganesan V, *Indian J Technol*, 18 (1980), 447-450.
16 Zhang X & Chiu H, *Int J Turbo Jet Engines*, 4 (1987) 251-262.
17 Chuang S H & Jiang J S, *Int J Numer Methods Fluids*, 11 (1990) 303-316.
18 Ravichandran M, *Experimental and theoretical investigations of afterburner*, Ph.D. Thesis, IC Engines Laboratory, Indian Institute of Technology Madras, Chennai, India, 1993.
19 Lee D & Lin J S, *Numer Heat Transf*, 20 (1991) Part A, 65-79.
20 Takashi Tamaru, *JSME Int J*, 39 (1996) Series B, No.1.